Journal of Sound and Vibration (1998) **209**(5), 797–810

FREE VIBRATION OF POLAR ORTHOTROPIC LAMINATED CIRCULAR AND ANNULAR PLATES

C.-C. Lin and C.-S. Tseng

Institute of Applied Mathematics, National Chung-Hsing University, Taichung, Taiwan, Republic of China

(*Received* 12 *June* 1996, *and in final form* 29 *August* 1997)

The paper deals with the free vibration analysis of polar orthotropic laminated circular and annular plates. The first order shear deformation theory and the variational energy method are employed in the mathematical formulation, and an eight-node isoparametric finite element model in polar co-ordinates is used for finding natural frequencies. The effects of material property, stacking sequence, hole size, plate thickness to radius ratio and boundary conditions on natural frequencies are investigated. Numerical results are shown in tabular and graphical forms, and some comparisons with existing results are made for the validation purpose.

1. INTRODUCTION

Numerous investigations on free vibration of elastic plates are available, but little has been done on the vibration of plates having polar orthotropy. Analytical solutions for natural frequencies of polar orthotropic circular and annular plates can only be obtained under some special conditions. Minkarah and Hoppman [1], Pandalai and Patel [2] investigated the natural frequencies of polar orthotropic circular and annular plates by analytical methods, but these studies are constrained to certain conditions such as a specific ratio of elastic constants (E_θ / E_r) or specific boundary conditions and so on. Analytical solutions have not been found for the general case so far. Vijayakumar and Ramaiah [3–5], Narita [6, 7] determined the natural frequencies of polar orthotropic circular and annular plates by using the Rayleigh–Ritz method. Using the finite difference technique, Greenberg and Stavsky [8] analyzed the natural frequencies of polar orthotropic laminated sandwich circular and annular plates with different materials and boundary conditions. Ginesu *et al*. [9] presented a finite element analysis for finding natural frequencies of polar orthotropic circular and annular plates with different boundary conditions; Gorman [10] also investigated the natural frequencies of polar orthotropic circular and annular plates by the finite element method. The studies mentioned above are all based on the classical plate theory. However, to the authors' knowledge, no known work exists on free vibration of polar orthotropic circular and annular plates including the transverse shear effect.

The essential purpose of this article is to investigate the free vibration of polar orthotropic laminated circular and annular plates by using a finite element model with first-order shear deformation theory.

0022–460X/98/050797 + 14 $25.00/0/sv971293

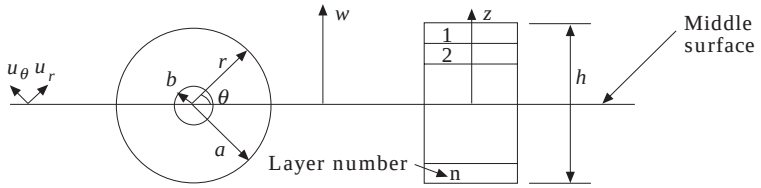

Figure 1. Geometry and co-ordinates of circular or annular plates.

2. MATHEMATICAL FORMULATION

The laminated plate of constant thickness h is composed of polar orthotropic laminae stacking symmetrically or antisymmetrically about the middle surface of plate. Polar co-ordinates (r, θ, z) are used for plate co-ordinates as shown in Figure 1, where u_r, u_θ, w denote the displacements of any point of the plate in the corresponding r, θ, z directions. The external forces acting on the plate are shown in Figure 2 in which q, $\bar{t}_n$, $\bar{t}_{ns}$, $\bar{t}_{nz}$, are the external forces, and n, s denote normal and tangential directions at the boundary of the plate, respectively.

A first-order shear deformation theory is employed, and the displacement field is assumed to be of the form

$$u_r(r, \theta, z, t) = u_r^0(r, \theta, t) + z\varphi_r(r, \theta, t),$$
$$u_\theta(r, \theta, z, t) = u_\theta^0(r, \theta, t) + z\varphi_\theta(r, \theta, t), \qquad w(r, \theta, z, t) = w(r, \theta, t). \tag{1}$$

where u_r^0, u_θ^0, w denote the displacements of any point on the middle surface, and φ_r, φ_θ are the rotations of the normal to the midplane about the θ, r-axes, respectively.

Strain-displacement relations are of the following form in polar co-ordinates

$$\varepsilon_r = \varepsilon_r^0 + z\kappa_r, \qquad \varepsilon_\theta = \varepsilon_\theta^0 + z\kappa_\theta, \qquad \gamma_{r\theta} = \gamma_{r\theta}^0 + z\kappa_{r\theta},$$
$$\gamma_{rz} = \gamma_{rz}^0$$
$$\gamma_{\theta z} = \gamma_{\theta z}^0, \tag{2}$$

where

$$\varepsilon_r^0 = u_{r,r}^0, \qquad \varepsilon_\theta^0 = (1/r)(u_{\theta,\theta}^0 + u_r^0), \qquad \varepsilon_\theta^0 = (1/r)(u_{\theta,\theta}^0 + u_r^0),$$
$$\gamma_{r\theta}^0 = (1/r)(u_{r,\theta}^0 - u_\theta^0) + u_{\theta,r}^0,$$
$$\gamma_{rz}^0 = \varphi_r + w_{,r}, \qquad \gamma_{\theta z}^0 = \varphi_\theta + (1/r)w_{,\theta}, \qquad \kappa_r = \varphi_{r,r},$$
$$\kappa_\theta = (1/r)(\varphi_{\theta,\theta} + \varphi_r), \qquad \kappa_{r\theta} = (1/r)(\varphi_{r,\theta} - \varphi_\theta) + \varphi_{\theta,r}. \tag{3}$$

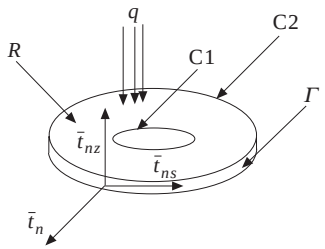

Figure 2. Loadings of circular or annular plates.

According to the shear deformation theory, the constitutive equations for the kth layer of a polar orthotropic laminated plate can be written in the following form in polar co-ordinates

$$\begin{Bmatrix}\sigma_r\\ \sigma_\theta\\ \tau_{r\theta}\end{Bmatrix}^{(k)} = \begin{bmatrix}Q_{11} & Q_{12} & 0\\ Q_{12} & Q_{22} & 0\\ 0 & 0 & Q_{66}\end{bmatrix}^{(k)} \begin{Bmatrix}\varepsilon_r\\ \varepsilon_\theta\\ \gamma_{r\theta}\end{Bmatrix}, \qquad \begin{Bmatrix}\tau_{rz}\\ \tau_{\theta z}\end{Bmatrix}^{(k)} = \begin{bmatrix}Q_{44} & 0\\ 0 & Q_{55}\end{bmatrix}^{(k)} \begin{Bmatrix}\gamma_{rz}\\ \gamma_{\theta z}\end{Bmatrix}, \tag{4}$$

where Q_{ij} are the stiffnesses of the material.

The stress resultants are defined as

$$\begin{bmatrix}N_r & M_r\\ N_\theta & M_\theta\\ N_{r\theta} & M_{r\theta}\end{bmatrix} = \int_{-h/2}^{h/2} \begin{Bmatrix}\sigma_r\\ \sigma_\theta\\ \tau_{r\theta}\end{Bmatrix} (1, z)\, \mathrm{d}z, \qquad \begin{bmatrix}Q_r\\ Q_\theta\end{bmatrix} = \int_{-h/2}^{h/2} \begin{Bmatrix}\tau_{rz}\\ \tau_{\theta z}\end{Bmatrix} \mathrm{d}z \tag{5}$$

Using equations (2) and (4) in (5), the constitutive equations of laminated plate become

$$\begin{bmatrix}N_r\\ N_\theta\\ N_{r\theta}\\ M_r\\ M_\theta\\ M_{r\theta}\end{bmatrix} = \begin{bmatrix}[A_{ij}] & [B_{ij}]\\ [B_{ij}] & [D_{ij}]\end{bmatrix} \begin{bmatrix}\varepsilon_r^0\\ \varepsilon_\theta^0\\ \gamma_{r\theta}^0\\ \kappa_r\\ \kappa_\theta\\ \kappa_{r\theta}\end{bmatrix}, \qquad \begin{bmatrix}Q_r\\ Q_\theta\end{bmatrix} = \begin{bmatrix}A_{44} & A_{45}\\ A_{45} & A_{55}\end{bmatrix} \begin{bmatrix}\gamma_{rz}^0\\ \gamma_{\theta z}^0\end{bmatrix},$$

$$i, j = 1, 2, 6. \tag{6}$$

where

$$(A_{ij} \quad B_{ij} \quad D_{ij}) = \int_{-h/2}^{h/2} Q_{ij}^{(k)}\, (1 \quad z \quad z^2)\, \mathrm{d}z, \qquad i, j = 1, 2, 6,$$

$$A_{ij} = k^2 \int_{-h/2}^{h/2} Q_{ij}^{(k)}\, \mathrm{d}z, \qquad (k^2 = 5/6) \qquad i, j = 4, 5, \tag{7}$$

in which $Q_{16}^{(k)}$, $Q_{26}^{(k)}$ and $Q_{45}^{(k)}$ are not included according to equation (4). The kinetic energy of a laminated plate is

$$T = \int\int\int_V \tfrac{1}{2}\rho(\dot{u}_r^2 + \dot{u}_\theta^2 + \dot{w}^2)\, \mathrm{d}V, \tag{8}$$

where ρ denotes mass density per unit volume, and the total potential energy of laminated plate is defined as

$$U = U_b + U_s + U_m + V_e, \tag{9}$$

where U_b is strain energy of bending, U_s is strain energy of shear, U_m is strain energy due to stress resultants N_r, N_θ, $N_{r\theta}$ induced by inplane forces in conjunction with additional

strains ε_r', ε_θ', $\gamma_{r\theta}'$ of middle surface due to deflection w, and V_e denotes the potential energy of external forces $(q, \bar{t}_n, \bar{t}_{ns}, \bar{t}_{nz})$. They are given as

$$U_b = \int\int\int_V \tfrac{1}{2}(\sigma_r \varepsilon_r + \sigma_\theta \varepsilon_\theta + \tau_{r\theta}\gamma_{r\theta})\,\mathrm{d}V, \qquad U_s = \int\int\int_V \tfrac{1}{2}(\tau_{rz}\gamma_{rz} + \tau_{\theta z}\gamma_{\theta z})\,\mathrm{d}V,$$

$$U_m = \int\int_R (N_R \varepsilon_r' + N_\theta \varepsilon_\theta' + N_{r\theta}\gamma_{r\theta}')\,\mathrm{d}A,$$

$$V_e = \left(-\int\int_R qw\,\mathrm{d}A\right) + \left[-\oint_\Gamma (\bar{t}_n u_n + \bar{t}_{ns} u_s + \bar{t}_{nz} w)\,\mathrm{d}\Gamma\right] \tag{10}$$

where R is the inplane region of the plate, and Γ is its boundary.

Applying the Hamilton's principle and the variational method, one may obtain the equations of motion

$$\begin{gathered}
N_{r,r} + (1/r)N_{r\theta,\theta} + (1/r)(N_r - N_\theta) = I_0 \ddot{u}_r^0 + I_1 \ddot{\varphi}_r, \\
N_{r\theta,r} + (1/r)N_{\theta,\theta} + (2/r)N_{r\theta} = I_0 \ddot{u}_\theta^0 + I_1 \ddot{\varphi}_\theta, \\
(Q_r + N_r w_{,r} + (1/r)N_{r\theta} w_{,\theta})_{,r} + (1/r)(Q_\theta + (1/r)N_\theta w_{,\theta} + N_{r\theta} w_{,r})_{,\theta} \\
+ (1/r)(Q_r + N_r w_{,r} + (1/r)N_{r\theta} w_{,\theta}) + q = I_0 \ddot{w}, \\
M_{r,r} + (1/r)M_{r\theta,\theta} + (1/r)(M_r - M_\theta) - Q_r = I_1 \ddot{u}_r^0 + I_2 \ddot{\varphi}_r, \\
M_{r\theta,r} + (1/r)M_{\theta,\theta} + (2/r)M_{r\theta} - Q_\theta = I_1 \ddot{u}_\theta^0 + I_2 \ddot{\varphi}_\theta,
\end{gathered} \tag{11}$$

where $(I_0, I_1, I_2) = \int_{-h/2}^{h/2} \rho(1, z, z^2)\,\mathrm{d}z$ and the subscript after a comma denotes partial differentiation with respect to the subscript variable.

The boundary conditions are specified in the form on C as

$$\begin{gathered}
\delta u_r^0 = 0 \quad \text{or} \quad \bar{N}_r = N_r, \qquad \delta u_\theta^0 = 0 \quad \text{or} \quad \bar{N}_{r\theta} = N_{r\theta}, \qquad \delta\varphi_r = 0 \quad \text{or} \quad \bar{M}_r = M_r, \\
\delta\varphi_\theta = 0 \quad \text{or} \quad \bar{M}_{r\theta} = M_{r\theta}, \qquad \delta w = 0 \quad \text{or} \quad \bar{Q}_r = Q_r + N_r w_{,r} + (1/r)N_{r\theta} w_{,\theta},
\end{gathered} \tag{12}$$

where C is the boundary line of the midplane, and $\bar{N}_r$, $\bar{N}_{r\theta}$, $\bar{M}_r$, $\bar{M}_{r\theta}$, $\bar{Q}_r$ are applied loads given at C.

3. FINITE ELEMENT ANALYSIS

The eight-node isoparametric element is used in the analysis for finding the natural frequencies. Since the geometry, material property and boundary conditions of the problems considered in this paper are axial symmetric, a quarter plate is taken as the analysis model for simplifying the problem.

If the quarter plate model is divided into n finite elements, then the Lagrange functional L is expressed as

$$L = \sum_{e=1}^{n} L_e (u_r^{0e}, u_\theta^{0e}, w^e, \varphi_r^e, \varphi_\theta^e). \tag{13}$$

The displacement field $\{d_e\}$ of any point in the element e can be expressed in terms of the nodal displacements $\{q_i^e\}$ of the element

$$\{d_e(r,\theta)\} = \sum_{i=1}^{8} [N_i]\{q_i^e\},$$

$$\{q_i^e\}^t = (u_{ri}^{0e}, u_{\theta i}^{0e}, w_i^e, \varphi_{ri}^e, \varphi_{\theta i}^e), \qquad \{d_e\}^{\mathrm{t}} = (u_r^{0e}, u_\theta^{0e}, w^e, \varphi_r^e, \varphi_\theta^e), \tag{14}$$

where $[N_i]$ is the ith interpolation (shape) function, and the superscript t denotes the matrix transpose.

With strain–displacement relations given in equations (1) and (2), one may obtain

$$\{\varepsilon_b^e\} = \sum_{i=1}^{8} [B_b^e]\{q_i^e\}, \qquad \{\varepsilon_b^e\}^{\mathrm{t}} = (\varepsilon_r^0, \varepsilon_\theta^0, \gamma_{r\theta}^0, \kappa_r, \kappa_\theta, \kappa_{r\theta}),$$

$$\{\varepsilon_s^e\} = \sum_{i=1}^{8} [B_s^e]\{q_i^e\}, \qquad \{\varepsilon_s^e\}^{\mathrm{t}} = (\gamma_{rz}^0, \gamma_{\theta z}^0), \tag{15}$$

where

$$[B_b^e] = \begin{bmatrix} \partial N_i/\partial r & 0 & 0 & 0 & 0 \\ (1/r)N_i & (1/r)\partial N_i/\partial\theta & 0 & 0 & 0 \\ (1/r)\partial N_i/\partial\theta & \partial N_i/\partial r - (1/r)N_i & 0 & 0 & 0 \\ 0 & 0 & 0 & \partial N_i/\partial r & 0 \\ 0 & 0 & 0 & (1/r)N_i & (1/r)\partial N_i/\partial\theta \\ 0 & 0 & 0 & (1/r)\partial N_i/\partial\theta & \partial N_i/\partial r - (1/r)N_i \end{bmatrix},$$

$$[B_s^e] = \begin{bmatrix} 0 & 0 & \partial N_i/\partial r & N_i & 0 \\ 0 & 0 & (1/r)\partial N_i/\partial\theta & 0 & N_i \end{bmatrix}, \tag{16}$$

where $[B_b^e]$ denotes the elemental strain matrix of bending, and $[B_s^e]$ denotes the elemental strain matrix of shear. It is noted that both $[B_b^e]$ and $[B_s^e]$ are not constants but are functions of r.

The following equation is derived by the aid of stress–displacement relations again

$$\{\sigma_b^e\} = \sum_{i=1}^{8} [D_b]\{\varepsilon_b^e\} = \sum_{i=1}^{8} [D_b]\,[B_b^e]\{q_i^e\},$$

$$\{\sigma_s^e\} = \sum_{i=1}^{8} [D_s]\{\varepsilon_s^e\} = \sum_{i=1}^{8} [D_s]\,[B_s^e]\{q_i^e\}, \tag{17}$$

where

$$[D_b] = \begin{bmatrix} A_{ij} & B_{ij} \\ B_{ij} & D_{ij} \end{bmatrix}, \qquad i,j = 1, 2, 6, \qquad [D_s] = \begin{bmatrix} A_{44} & A_{45} \\ A_{45} & A_{55} \end{bmatrix}.$$

Free flexural vibration for small deformation of plates without inplane loading are dealt within this study. The stretching of middle surface due to w is negligible and thus only

the strain energies due to bending and shear are accounted for. Other terms of U_m and V_e in equation (10) are omitted.

Strain energies due to bending and shear of any plate element e are given as

$$U_b^e = \tfrac{1}{2}\int\int_{R_e} \{\varepsilon_b^e\}^{\mathrm{t}}[D_b]\{\varepsilon_b^e\}\,\mathrm{d}R_e = \tfrac{1}{2}(\{q_i^e\}^{\mathrm{t}}[K_b^e]\{q_i^e\}),$$

$$U_s^e = \tfrac{1}{2}\int\int_{R_e} \{\varepsilon_s^e\}^{\mathrm{t}}[D_s]\{\varepsilon_s^e\}\,\mathrm{d}R_e = \tfrac{1}{2}(\{q_i^e\}^{\mathrm{t}}[K_s^e]\{q_i^e\}), \tag{18}$$

and the kinetic energy of any plate element e is written as

$$T^e = \tfrac{1}{2}\int\int_{R_e} (\{\dot{q}_i^e\}^{\mathrm{t}}[N_i]^{\mathrm{t}})\,[I]\,([N_i]\{\dot{q}_i^e\})\,\mathrm{d}R_e = \tfrac{1}{2}(\{\dot{q}_i^e\}^{\mathrm{t}}[M^e]\{\dot{q}_i^e\}), \tag{19}$$

where

$$[I] = \begin{bmatrix} I_0 & 0 & 0 & I_1 & 0 \\ & I_0 & 0 & 0 & I_1 \\ & & I_0 & 0 & 0 \\ & \text{sym} & & I_2 & 0 \\ & & & & I_2 \end{bmatrix}, \qquad [K_b^e] = \int\int_{R_e} [B_b^e]^{\mathrm{t}}[D_b]\,[B_b^e]\,\mathrm{d}R_e,$$

$$[K_s^e] = \int\int_{R_e} [B_s^e]^{\mathrm{t}}[D_s]\,[B_s^e]\,\mathrm{d}R_e, \qquad [M^e] = \int\int_{R_e} [N_i]^{\mathrm{t}}[I]\,[N_i]\,\mathrm{d}R_e. \tag{20}$$

Since it is difficult to integrate equation (20) directly according to the isoparametric element formulation, the global coordinate system (r, θ) is transformed to the local co-ordinate system (ξ, η). Then equation (20) takes the following form

$$[K_b^e] = \int_{-1}^{1}\int_{-1}^{1} [B_b^e]^{\mathrm{t}}[D_b]\,[B_b^e]\,\det|J|\,\mathrm{d}\xi\,\mathrm{d}\eta,$$

$$[K_s^e] = \int_{-1}^{1}\int_{-1}^{1} [B_s^e]^{\mathrm{t}}[D_s]\,[B_s^e]\,\det|J|\,\mathrm{d}\xi\,\mathrm{d}\eta,$$

$$[M^e] = \int_{-1}^{1}\int_{-1}^{1} [N_i]^{\mathrm{t}}[I]\,[N_i]\,\det|J|\,\mathrm{d}\xi\,\mathrm{d}\eta, \tag{21}$$

where J is the Jacobian matrix given by $J(\xi, \eta) = [\partial(r, \theta)/\partial(\xi, \eta)]$. As mentioned before, $[B_b^e]$ and $[B_s^e]$ are not constants but are functions of r. Although Guassian quadrature is capable of dealing with the variable radius r, for simplicity of integrations involved in equation (21), a suitable constant radius $\bar{r}^e$ is selected to replace the variable radius r in the strain matrices. In this paper, $\bar{r}^e = (r_{min}^e + r_{max}^e)/2$ is chosen, which is the mean value between the minimum radius and maximum radius of plate element e.

Assembling the following strain energy of bending U_b and U_s, and kinetic energy T of the n elements, they are

$$U_b = \sum_{e=1}^{n} U_b^e = \tfrac{1}{2} \sum_{e=1}^{n} \{q_i^e\}^t [K_b^e] \{q_i^e\} = \tfrac{1}{2} \{\Delta\}^t [K_b^e] \{\Delta\},$$

$$U_s = \sum_{e=1}^{n} U_s^e = \tfrac{1}{2} \sum_{e=1}^{n} \{q_i^e\}^t [K_s^e] \{q_i^e\} = \tfrac{1}{2} \{\Delta\}^t [K_s^e] \{\Delta\},$$

$$T = \sum_{e=1}^{n} T^e = \tfrac{1}{2} \sum_{e=1}^{n} \{\dot{q}_i^e\}^t [M^e] \{\dot{q}_i^e\} = \tfrac{1}{2} \{\dot{\Delta}\}^t [M^e] \{\dot{\Delta}\}, \tag{22}$$

where $\{\Delta\}^t = [\{u_r^0\}^t, \{u_\theta^0\}^t, \{w\}^t, \{\varphi_r\}^t, \{\varphi_\theta\}^t]$ is a $5m \times 1$ column vector with m being the number of total nodal points, which denotes the global displacement vector of laminated plates.

Again, applying the Hamilton's principle in conjunction with the variational method

$$\delta \int_{t1}^{t2} L \, \mathrm{d}t = \delta \int_{t1}^{t2} (\{\Delta\}^t [K_b] \{\Delta\}) + \{\Delta\}^t [K_s] \{\Delta\} - \{\dot{\Delta}\}^t [M] \{\dot{\Delta}\}) \, \mathrm{d}t = 0, \tag{23}$$

one arrives at

$$\int_{t1}^{t2} ([M] \{\ddot{\Delta}\} + [K] \{\Delta\}) \, \delta \{\Delta\}^t \, \mathrm{d}t = 0, \qquad [K] = [K_b] + [K_s]. \tag{24}$$

The equation of motion can be derived directly from equation (24), which is

$$[M] \{\ddot{\Delta}\} + [K] \{\Delta\} = 0. \tag{25}$$

For free vibration, the motion is assumed to be simple harmonic for each mode, i.e., $\{\Delta\} = \{\overline{\Delta}\} \, \mathrm{e}^{\mathrm{i}\omega t}$. Hence equation (25) can be rewritten in the form

$$([K] - \omega^2 [M]) \{\overline{\Delta}\} = 0, \tag{26}$$

and the natural frequencies can be determined from the following determinant

$$\mathrm{Det} \, |[K] - \omega^2 [M]| = 0, \tag{27}$$

where ω denotes the natural frequency of laminated plates, and the corresponding solutions of $\{\overline{\Delta}\}$ in equation (26) describes the vibration mode.

4. NUMERICAL RESULTS AND DISCUSSIONS

Exploiting the axisymmetric characteristics on the fundamental natural frequency and the corresponding mode shape, only one quadrant of plate is modelled. The whole plate mesh should be taken when investigating the higher modes of vibration. The boundary conditions and finite element mesh of the plate are shown in Figure 3. When b is very small in comparison with a, say $b/a = 0{\cdot}00001$, then the annular plate can be considered as a circular plate. In this paper, calculations for circular plates are simulated with this assumption to avoid the singularity at the origin ($r = 0$) when integrations are made.

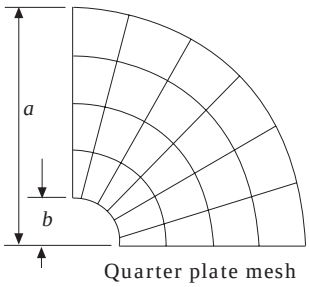

Figure 3. Finite element mesh and boundary conditions. Boundary conditions: clamped circular plate; $u_r^0 = u_\theta^0 = w = \varphi_r = \varphi_\theta = 0$ at $r = a$; simply supported circular plate, $\bar{N}_r = u_\theta^0 = w = \varphi_r = M_r = 0$ at $r = a$; C–C annular plate; $u_r^0 = u_\theta^0 = w = \varphi_\theta = 0$ at $r = a,\ b$; S–C annular plate, $\bar{N}_r = u_\theta^0 = w = \varphi_r = \bar{M}_r = 0$ at $r = b$, $u_r^0 = u_\theta^0 = w = \varphi_r = \varphi_\theta = 0$ at $r = a$; F–C annular plate, $\bar{N}_r = \bar{N}_{r\theta} = \bar{M}_r = \bar{M}_{r\theta} = \bar{Q}_r = 0$ at $r = b$.

A subspace iteration method [11] is applied to determine the eigenvalues and eigenvectors. According to the results of program executions, it took less than 10 iterations to reach convergent eigenvalues.

The parameters of materials are divided into two groups which are listed in Tables 1 and 2. It can be seen from Table 1 that materials I, II and III are different; whereas in Table 2, IV and V are of the same composite material but their fiber orientations along the radial and the circumferential directions are reversed.

To verify the algorithm and calculations made in this paper, comparisons between the present results and those of existing results based on the classical plate theory are made.

TABLE 1

Material property for materials I *to* III

Materials	E_θ / E_r	$E_{r\theta} / E_r$	E_{rz} / E_r	$E_{\theta z} / E_r$	$v_{\theta r}$	ρ
I	2	0·35	0·292	0·292	0·3	1·0
II	5	0·35	0·292	0·292	0·3	1·0
III	50	0·6613	0·5511	0·5511	0·26	1·0

TABLE 2

Material properties for materials IV *and* V. (*Ultra high modulus graphite epoxy*)

Materials	E_r (N/m^2)	E_θ (N/m^2)	$E_{r\theta}$ (N/m^2)	$v_{r\theta}$	ρ (kg/m^3)
IV	31×10^{10}	$0{\cdot}62 \times 10^{10}$	$0{\cdot}41 \times 10^{10}$	0·26	$1{\cdot}613 \times 10^3$
V	$0{\cdot}62 \times 10^{10}$	31×10^{10}	$0{\cdot}41 \times 10^{10}$	0·0052	$1{\cdot}613 \times 10^3$

TABLE 3

Fundamental natural frequencies ($\lambda = \omega a^2\sqrt{\rho h/D}$) *of clamped isotropic* ($v = 0{\cdot}3$) *circular plates*

h/a	present (SDT)	(Raleigh-Ritz) [12]	Analytical (CPT)
0·05	10·047	10·145	–
0·1	9·812	9·941	–
0·15	9·453	9·629	10·216
0·2	9·016	9·240	–
0·25	8·536	8·807	–

TABLE 4

Fundamental natural frequencies ($\lambda = \omega a^2\sqrt{\rho h/D}$) *of clamped–clamped isotropic* ($\nu = 0{\cdot}3$) *annular plates*

b/a	a/h	present (SDT)	(CPT, FEM) [13]	Analytical (CPT)
0·1	10	24·480	–	–
	40	27·466	27·295	27·281
	100	27·585	–	–
0·3	10	38·621	–	–
	40	45·143	45·371	45·346
	100	45·406	–	–
0·5	10	67·934	–	–
	40	88·069	89·299	89·251
	100	89·034	–	–

As shown in Table 3, the present results and those obtained by Irie *et al*. [12] for clamped isotropic circular plates are in good agreements. Excellent agreements between the present results and those of Pardoen's [13] for clamped–clamped isotropic annular plates are also shown in Table 4. In Figure 4, effects of the thickness on the fundamental frequency of clamped polar orthotropic circular plates are compared with those using the classical plate theory by Narita [7]. As expected, excellent agreements are obtained when the plate is thin. However, large discrepancy occurred when the plate thickness becomes larger, especially for plates clamped at the center point. Results of polar orthotropic annular plates with a free inner edge and a clamped outer edge are compared with those obtained by Vijayakumar and Ramaiah [4] using the classical plate theory, as shown in Figure 5. It shows that results based on the classical plate theory give significant errors when $a/h \leqslant 20$. All of these comparisons show that the present model is reliable and effective for isotropic/polar orthotropic circular or annular thin plates.

Fundamental natural frequencies of polar orthotropic laminated circular plates with clamped and simply supported boundary conditions are listed in Table 5. Results show that natural frequencies are influenced by stacking sequence, the order of the magnitude of the fundamental frequency for the five different laminates being

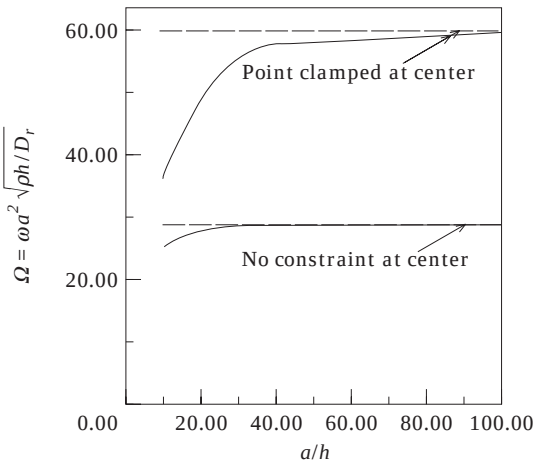

Figure 4. Fundamental frequencies versus thickness ratio of clamped polar orthotropic circular plates (material III). Key: — —, [7]; ——, present.

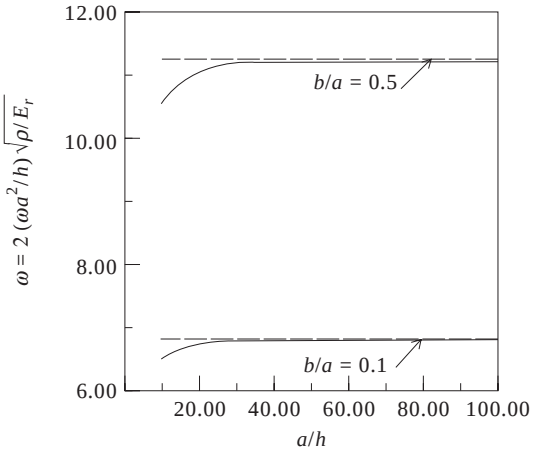

Figure 5. Fundamental frequencies versus thickness ratio of free–clamped polar orthotropic annular plates (material I). Key: — —, [4]; ——, present.

(III) > (III/II/II/III) > (III/II/III/II) > (II/III/III/II) > (II). For annular plates, the effects of stacking sequence on natural frequencies when the outer edge is clamped and the inner edge is either clamped, simply supported or free are illustrated in Table 6, and are similar to those for circular plates. It is noted that the free–clamped annular plate can be regarded as a clamped circular plate with a free hole. Effects of the hole of the fundamental frequency of clamped circular plates are shown in Figure 6. It shows that the fundamental frequency increases as the size of the hole increases for all stacking sequences considered.

Another class of laminated circular or annular plates composed of polar orthotropic laminae made of the same composite material with their fiber orientated in either the radial or circumferential direction is considered. The ultra-high modulus graphite epoxy composites are used in the examples. Material IV has fibers arranged along the radial direction and material V has fibers arranged along the circumferential direction. Results on the fundamental frequency of several polar orthotropic laminated circular plates with clamped or simply supported boundary conditions are shown in Table 7. They reveal that among these different stacking sequences, the smallest natural frequency occurs when the plate is composed of laminae which are made of material V only. It seems to be reasonable, since the displacement and curvature of the first vibration mode of plates are varied in

TABLE 5

Fundamental frequencies ($\Lambda = \omega a^2\sqrt{\rho h/D_{11}}$) *of polar orthotropic laminated circular plates with clamped and simply supported boundary conditions*

BC	a/h	(III)	(II)	(III/II/III/II)	(III/II/II/III)	(II/III/III/II)
Clamped	10	25·807	12·998	19·782	23·422	15·864
	20	27·736	13·665	21·456	26·309	16·706
	50	28·644	13·872	22·008	27·331	16·967
	100	28·781	13·902	22·090	27·487	17·006
S–S	10	21·206	8·546	15·602	19·758	11·365
	20	22·800	8·816	16·467	21·457	11·755
	50	23·446	9·026	16·867	22·145	12·001
	100	23·628	9·139	17·011	22·337	12·114

TABLE 6

Fundamental frequencies ($\Lambda = \omega a^2\sqrt{\rho h/D_{11}}$) *of polar orthotropic laminated annular plates*

BC	b/a	a/h	(III)	(II)	(III/II/III/II)	(III/II/II/III)	(II/III/III/II)
C–C	0·1	10	43·231	26·865	35·844	39·740	31·344
		20	54·224	30·914	43·616	50·977	36·044
		50	59·824	32·461	47·156	57·101	37·857
		100	60·811	32·710	47·754	58·214	38·150
	0·5	10	84·977	66·057	75·706	79·266	72·661
		20	102·623	82·416	92·216	98·656	87·009
		50	110·036	89·776	99·272	107·374	92·916
		100	111·239	91·002	100·425	108·826	93·867
S–C	0·1	10	43·023	25·558	35·497	39·557	30·557
		20	53·722	28·381	42·901	50·495	34·771
		50	59·117	30·030	46·226	56·382	36·364
		100	60·065	30·220	46·785	57·448	36·620
	0·5	10	76·596	54·319	65·559	71·644	59·979
		20	88·679	63·002	75·585	84·914	67·735
		50	93·307	66·337	79·362	90·250	70·557
		100	94·033	66·860	79·987	91·102	70·911
F–C	0·1	10	25·743	13·526	21·107	23·791	16·152
		20	28·410	13·936	21·798	26·670	17·007
		50	29·053	14·147	22·356	27·727	17·273
		100	29·193	14·178	22·440	27·886	17·313
	0·5	10	37·329	20·636	30·173	35·010	24·751
		20	41·246	21·851	32·847	39·320	26·204
		50	42·591	22·233	33·737	40·850	26·662
		100	42·794	22·290	33·870	41·084	26·730

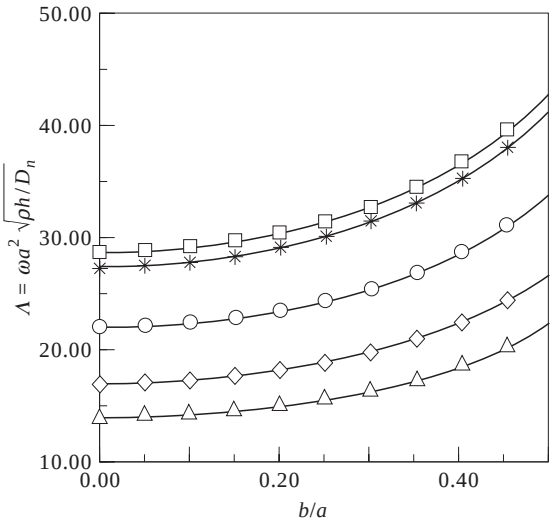

Figure 6. Fundamental frequencies of different clamped polar orthotropic circular plates with free holes, ($a/h = 20$). Key: —□—, stacking all III; —△—, stacking all II, —○—, stacking III/II/III/II; —*—, stacking III/II/II/III; —◇—, stacking II/III/III/II.

TABLE 7

Fundamental frequencies ($f = \omega a^2\sqrt{\rho h/D_{66}}$) *of polar orthotropic laminated circular plates with clamped and simply supported boundary conditions*

BC	a/h	(IV)	(V)	(V/IV/V/IV)	(IV/V/V/IV)	(V/IV/IV/V)
Clamped	10	44·836	30·871	42·587	45·919	38·250
	20	56·479	34·143	52·433	58·869	44·991
	50	61·639	35·247	56·653	64·886	47·618
	100	62·489	35·416	57·341	65·897	48·623
S–S	10	26·095	9·574	24·097	26·963	18·844
	20	28·057	9·917	25·699	29·173	19·676
	50	28·851	10·316	26·388	30·111	20·118
	100	29·075	10·566	26·614	30·397	20·306

the radial direction only. Hence, the laminated plate having higher stiffness in the radial direction would produce higher natural frequency and vice versa. Because the fibers of material V are placed along the circumferential direction, the stiffness in the radial direction for the material V laminate is smaller than any other laminates. As a result, the natural frequency of laminated plate made of pure material V is the lowest of all laminated plates. The major difference from the former example is that the effect of stacking sequence on the fundamental frequency is no longer the same. The order of the magnitude of the fundamental frequency for these five different types of laminates is (IV/V/V/IV) > (IV) > (V/IV/V/IV) > (V/IV/IV/V) > (V). Here one observes that the fundamental frequency of (IV/V/V/IV) laminated plate is higher than the (IV) laminate. The same interesting behavior had been found for sandwich plates by Greenberg and Stavsky [8]. Fundamental frequencies of C–C, S–C and F–C polar orthotropic laminated annular plates are listed in Table 8. It shows that the same trend of the order of the magnitude

TABLE 8

Fundamental frequencies ($f = \omega a^2\sqrt{\rho h/D_{66}}$) *of polar orthotropic laminated annular plates*

BC	b/a	a/h	(IV)	(V)	(V/IV/V/IV)	(IV/V/V/IV)	(V/IV/IV/V)
C–C	0·1	10	80·76	53·19	74·93	80·04	66·23
		20	136·32	66·73	114·70	133·29	91·64
		50	200·00	73·62	147·05	191·23	107·61
	0·5	10	161·00	104·63	156·51	160·53	144·42
		20	302·89	126·33	276·10	299·76	222·54
		50	564·15	135·45	431·90	544·61	283·73
S–C	0·1	10	78·96	52·94	73·00	78·23	65·22
		20	125·48	66·11	105·88	122·71	88·29
		50	165·35	72·75	127·66	159·26	101·85
	0·5	10	155·83	94·29	148·77	154·92	140·12
		20	278·56	109·16	244·22	273·96	156·39
		50	457·39	114·86	338·82	438·61	166·20
F–C	0·1	10	46·13	31·35	43·20	46·38	39·01
		20	58·42	34·63	53·00	59·03	45·88
		50	63·94	35·75	57·16	64·78	48·55
	0·5	10	80·43	45·95	70·78	79·18	60·36
		20	118·28	50·77	92·46	114·33	72·25
		50	143·12	52·43	102·99	136·24	77·03

of the fundamental frequency as those of circular plates only takes place when the boundary condition is free–clamped and the hole–radius ratio $b/a = 0{\cdot}1$. Whereas for the other cases, the order of the magnitude of the fundamental frequency for these five laminates is (IV) > (IV/V/V/IV) > (V/IV/V/IV) > (V/IV/IV/V) > (V). This is quite different from that for circular plates.

5. CONCLUSIONS

The fundamental natural frequency of polar orthotropic laminated plates has been estimated by employing the first order shear deformation theory and the eight-node isoparametric finite element technique. With the numerical results obtained, several conclusions are reached.

1. The present analytical method established systematically in polar co-ordinates is reliable and effective for finding natural frequencies and mode shapes of polar orthotropic circular and annular plates.

2. The fundamental frequency of polar orthotropic laminated circular plates with free hole increases as the hole size increases.

3. Transverse shear effects are more significant for polar orthotropic laminated plates than isotropic plates. Furthermore, the transverse shear effect are much more apparent for annular plates.

4. For polar orthotropic laminated circular plates or plates with a small free hole, the laminates (say IV/V/V/IV) stacked with outer layers having fibers along the radial direction and inner layers having fibers along the circumferential direction may have an higher fundamental frequency than the laminate stacked with all layers having fibers along the radial direction. However, for polar orthotropic laminated annular plates with inner edge constrained, the laminate stacked with all layers having fibers along the radial direction always has the highest fundamental frequency. The possible reason for these phenomena is that the circumferential stiffness in the central region makes a significant contribution to the vibration mode.

REFERENCES

1. L. A. Minkarah and H. Hoppman 1964 *Journal of the Acoustical Society of America* **36**, 470–475. Flexural vibration of cylindrically aerolotropic plates.
2. K. A. V. Pandalai and Sharad A. Patel 1965 *AIAA Journal* **3**, 780–781. Natural frequencies of orthotropic circular plates.
3. K. Vijayakumar and G. K. Ramaiah 1972 *Journal of Sound and Vibration* **24**, 165–175. On the use of a co-ordinate transformation for analysis of axisymmetric vibration of polar orthotropic annular plates.
4. K. Vijayakumar and G. K. Ramaiah 1973 *Journal of Sound and Vibration* **26**, 517–531. Natural frequencies of polar orthotropic annular plates.
5. K. Vijayakumar and G. K. Ramaiah 1974 *Journal of Sound and Vibration* **32**, 265–278. Estimation of higher natural frequencies of polar orthotropic annular plates.
6. Y. Narita 1984 *Journal of Sound and Vibration* **92**, 33–38. Natural frequencies of completely free annular and circular plates having polar orthotropy.
7. Y. Narita 1984 *Journal of Sound and Vibration* **93**, 503–511. Vibration of continuous polar orthotropic annular and circular plates.
8. J. B. Greenberg and Y. Stavsky 1979 *Journal of Acoustical Society of America* **66**, 501–508. Flexural vibration of certain full and annular composite orthotropic plates.
9. F. Ginesu, B. Picasso and P. Priolo 1979 *Journal of Sound and Vibration* **65**, 97–105. Vibration analysis of polar orthotropic annular discs.
10. D. G. Gorman 1983 *Journal of Sound and Vibration* **86**, 47–60. Natural frequencies of transverse vibration of polar orthotropic variable thickness annular plates.

11. K. J. BATHE 1982 *Finite element procedures in engineering analysis*. New York: Prentice-Hall.
12. T. IRIE, G. YAMADA and S. AOMURA 1980 *Journal of Applied Mechanics* **47**, 652–655. Natural frequency of Mindlin circular plates.
13. GERARD C. PARDOEN 1973 *Computers & Structures* **3**, 355–375. Static vibration and buckling analysis of axisymmetric circular plates using finite elements.